Received June 28, 2020, accepted July 1, 2020, date of publication July 16, 2020, date of current version July 30, 2020.

Digital Object Identifier 10.1109/ACCESS.2020.3008540

Compact UHF/VHF Monopole Antennas for CubeSats Applications

XIANG ZHANG[1], FU SUN[2], GUOXUAN ZHANG[2], AND LIMING HOU[1]
[1]School of Mechanical Engineering, Nanjing University of Science and Technology, Nanjing 210094, China
[2]College of Electronic Information Engineering, Nanjing University of Aeronautics and Astronautics, Nanjing 211106, China

Corresponding author: Xiang Zhang (zhxiang2002@126.com)

ABSTRACT In this paper, two compact monopole antennas working at 149 MHz (VHF) and 398 MHz (UHF) are proposed for CubeSats applications. Two monopole antennas are integrated on a double layer ceramic substrate. The overall dimensions of the folded antenna are 101 mm ×40 mm ×8.9 mm which is very small. Meander-line technique and foldable structure are proposed to achieve a compact design. The introduction of decoupling structure solves the problem of high coupling caused by small size. Computer simulations and measurements are conducted. The results demonstrate that the proposed design is a very promising candidate for CubeSats applications.

INDEX TERMS UHF/VHF, CubeSats, monopole antenna, meander-line, foldable structure, decoupling structure.

I. INTRODUCTION

CubeSat is a tiny cube-shaped satellite with dimensions of $10 \times 10 \times 10\ cm^3$ and a weight less than 1 kg [1]. Due to the low costs for manufacturing and launching, the range of applications has been extended rapidly, attracting military, commercial and academic interest. Antennas on a CubeSat may have different frequency bands, which vary from VHF band to millimeter wave band. Up to now, various antenna systems have been proposed. Structures of these antennas include linear wires, reflectors, deployable membranes, horns, and patches [2]. In most of the satellites, two sets of dipole antennas (UHF) and two sets of monopoles (VHF) are normally used for transmitting and receiving purpose respectively. The main concerns are the shadows from the solar panels [3], the mechanical complexity, and the limited space in the deployable system, which make it a complex design problem in the antenna design.

A number of antennas dedicated to satellite applications have been proposed. A single monopole antenna matched at two different frequencies is proposed in [4]. The antenna feeds a duplexer that separates the transmitting and receiving frequencies, which simplified the antenna system of a CubeSat. While conventional standard dipole antennas are too big to fit into a CubeSat, a deployable dipole/monopole is introduced in [5]. The Compass-2 satellite from RWTH Aachen [6] uses S-band for high-speed communication and a combined VHF/UHF system as a fallback solution for basic telemetry data. In this particular system, a UHF dipole antenna is combined with a VHF monopole antenna. The KNACKSAT mission by King Mongkut's University of Technology Bangkok [7] uses two perpendicular dipole antennas for each frequency band. In [8], the use of CubeSat body as an UHF antenna was proposed. The antenna does not rely on any deployable mechanical system, which increases the reliability of the satellite significantly. A CubeSat circularly polarized (CP) patch antenna system operating in L band and a method of efficient patch antenna stowage have been proposed in [9]. One antenna consists of two patch elements placed on separate solar-panel wings and interleaved while the wings are stowed. In [10], compact UHF patch antenna compatible with any CubeSat is proposed. The design involves a different combination of miniaturization techniques of patch antennas like folded meander line, partial ground plane, and shorting pin for small satellite applications.

In this paper, The UHF and VHF antennas are integrated into a compact structure. Miniaturized antenna size and low coupling are realized. To achieve a compact dimension, UHF antenna uses folded meander line which is designed on one side of the substrate and VHF antenna uses deployable structure. The decoupling structure design reduces the coupling between the two antennas, and finally a better effect is achieved. In order to simplify the antenna feeding circuit,

The associate editor coordinating the review of this manuscript and approving it for publication was Yasar Amin.

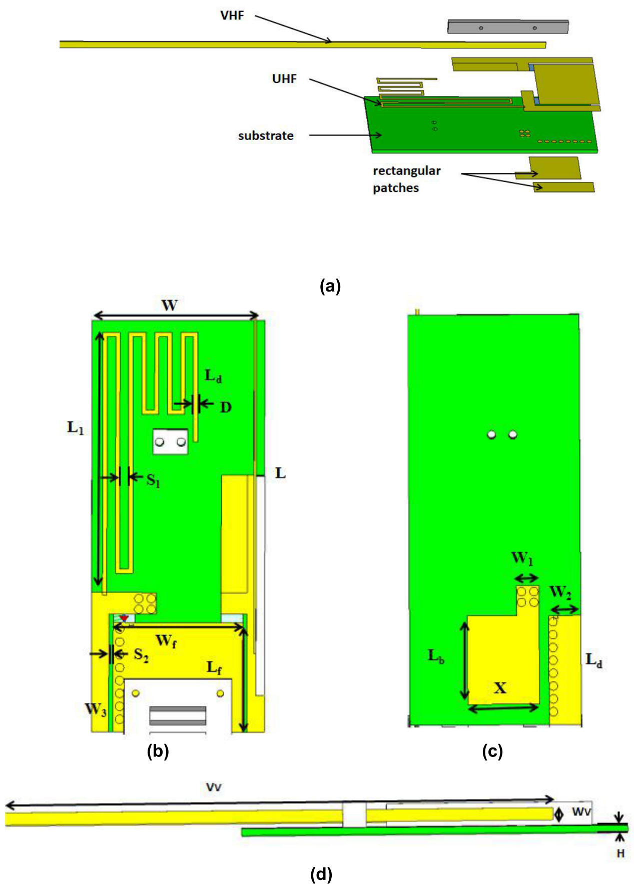

FIGURE 1. The configuration of the proposed antenna. (a) Exploded view (b) Top view (c) Bottom view (d) Side view.

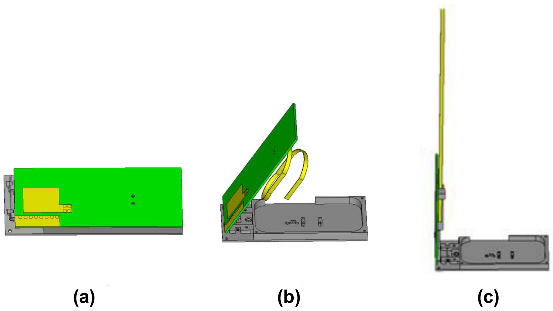

FIGURE 2. Schematic diagram of antenna expansion process. (a) fold state (b) Semi-expanded state (c) deployable state.

double-feed structure is designed. Compact profile makes the antenna have a wide range of applications in CubeSat.

After optimizing the antenna parameters, a prototype is fabricated and measured on a CubeSat. The paper is organized as follows. Section II introduces the antenna structure and design process. Section III discusses the results of the simulation and measurement. Section IV designs a decoupling structure. Section V concludes the paper.

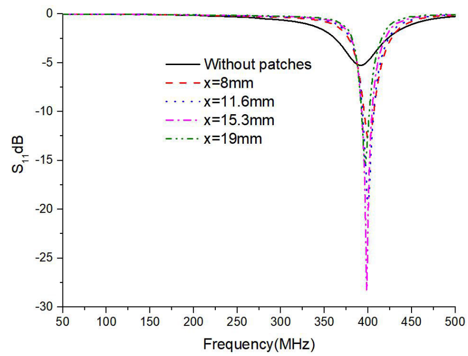

FIGURE 3. Simulated S_{11} with different values of x.

II. CONFIGURATION AND DESIGN

The configuration of the proposed antenna is shown in Figure 1. It consists of two driven monopoles, rectangular dielectric substrate, ground plane, two rectangular patches, and feeder circuit. The dimension of rectangular dielectric substrate is 95.78 mm $\times$ 40 mm $\times$ 1.6 mm. Two monopoles are integrated on the substrate. To achieve a compact structure, different miniaturization techniques are preferred in this design. For the UHF monopole working at 398 MHz, meander-line technique [11], [12] is implemented. The use of meander-line technique plays a role in reducing the antenna size. When the electromagnetic wave is fed into the antenna structure from the feed point, the current in the adjacent vertical branch of the curved polyline is in the opposite direction. Due to the coupling between adjacent lines and the bending angle effect, the electric length of the bent antenna is slightly less than the total length of the bent antenna, and the resonance frequency of the bent antenna is much lower than that of the unmodified monopole. The overall of the meander-line is equivalent to an inductive element, so two capacitive rectangular patches are placed on the back of the substrate to fine-tune the resonant frequency of the antenna to some extent. The parameter optimization simulation of rectangle patch width is carried out, as show in the Figure 3. When the size of rectangular patch gradually decreases, the matching effect of the antenna at 401 MHz becomes worse. The capacitive compensation of rectangular patches can be proved. For the VHF monopole, a $\lambda/4$ resonant monopole antenna at 149 MHz would require dimensions of 500 mm. It is obviously unreasonable to place the antenna upright before launch. Based on this consideration, we choose flexible materials that can be expanded. The antenna would be folded into the CubeSat body and deployed [13] in space. Figure 2 shows the unfolding progress of the antenna. Before the satellite is launched, the antenna is tied with a bundling rope make the antenna closed. When the satellite enters space, the fuse is used to fuse the corresponding binding rope at the anchor type base and the antenna is expanded accordingly. As the two monopole antennas are integrated together, there is a degree of coupling when antennas are working. The S_{21} curve of the proposed antenna is shown in the Figure 4. The isolation degree of UHF antenna is about -5 dB operating at

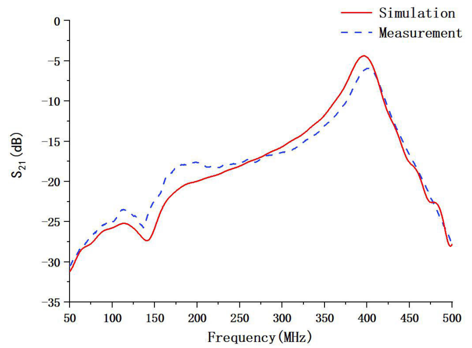

FIGURE 4. S_{21} curve of proposed antenna. UHF is port 1 and VHF is port 2.

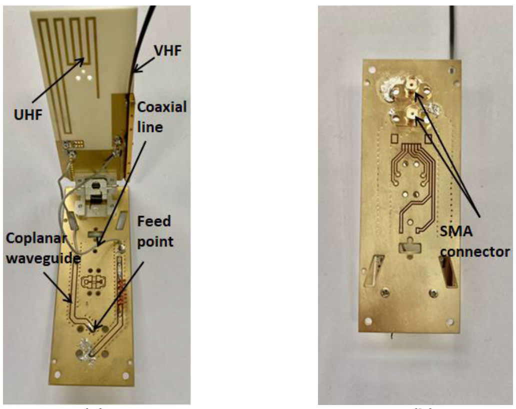

(a) (b)

FIGURE 5. The prototype of the proposed antenna. (a) Top view (b) Bottom View.

TABLE 1. Optimised antenna design parameters.

Name	Value	Name	Value
L	95.78	D	1
W	40	W_3	4
L_1	61.1	X	16.8
H	1.6	L_f	25.5
W_1	5.3	W_f	30
L_2	30.5	W_2	7.5
S_1	2	L_d	25.5
W_V	3	L_b	20.7
L_d	25.5	V_V	480

398 MHz and the isolation degree of VHF antenna is −26 dB operation at 149 MHz. In the later section, the coupling effect between the two antennas will be explained and a decoupling structure will be introduced.

All dimensions in millimetres.

In the simulation software, two discrete feed ports are set in the antenna, but special feed circuits is designed in the actual antenna, as shown in the Figure 5. The feed circuit includes two coplanar waveguide transmission lines on the PCB and two flexible coaxial lines. Two 50-ohm SMA connectors are soldered to the coplanar waveguide structure on the

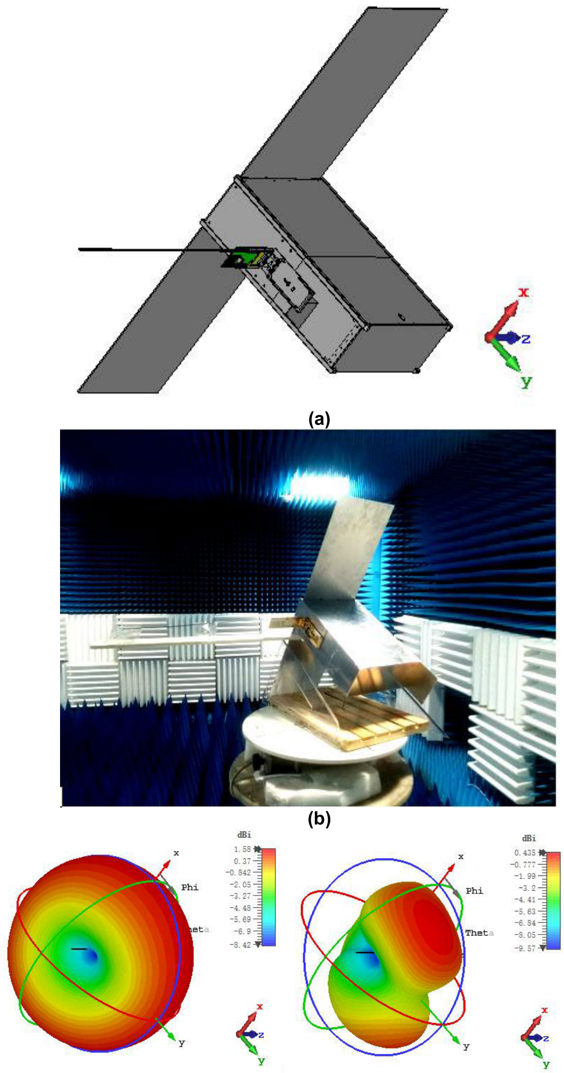

(c)

FIGURE 6. Antenna model with CubeSats. (a) Simulation (b) Measurement (c) The direction diagram under this perspective, operating at 149 MHz and 401 MHz respectively.

PCB board. Then use two flexible coaxial lines to connect the feed port of the antenna and the coplanar waveguide to realize feeding to the antennas In practical antenna debugging, impedance matching can be achieved by adding winding coils to the coplanar waveguide structure.

III. ANTENNA MEASUREMENTS

To verify the design, the antenna with optimized dimensions is fabricated and the prototype is shown in Figure 5. Final optimized design parameter of the realized antenna geometric layout is presented in Table 1. The performance of the UHF\VHF antenna is calculated.

A prototype of proposed antenna is fabricated and attached to the CubeSats structure as shown in Figure 6 (a) (b). Figure 6 (c) shows the radiation patterns of the proposed antenna at the same angle. The reflection coefficient of the proposed. UHF/VHF antenna has been measured using

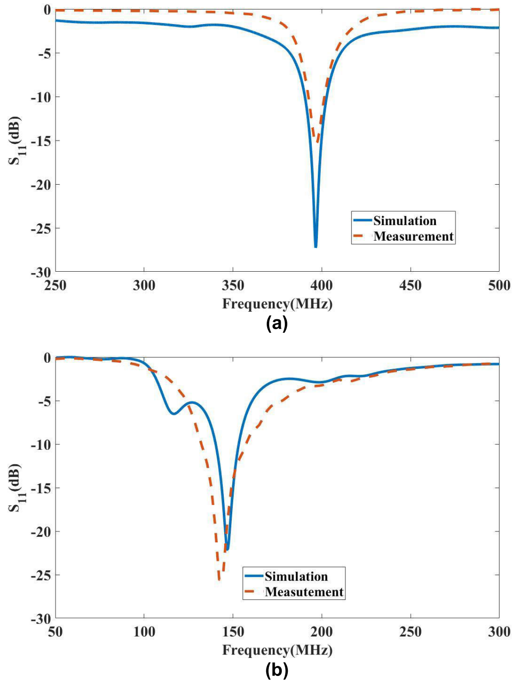

FIGURE 7. Simulated and Measured reflection coefficients of antenna with satellite structure (a) UHF (b) VHF.

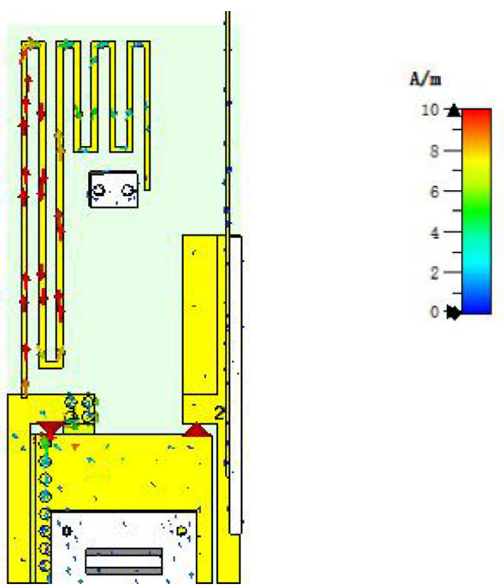

FIGURE 8. Surface current distribution of the UHF antenna.

Vector Network Analyzer (VNA). The simulated and measured antenna reflection coefficients are reported in Figure 7. The two results are in good agreement showing that a good matching has been obtained around the operating frequency. Figure 7 (a) shows the measured and simulated resonant frequencies of UHF antenna are all at 398 MHz; while the impedance bandwidth ($|S_{11}| < 10$ dB) is about 10 MHz. It can also be observed that measured and simulated resonant frequencies of VHF antenna are all at 149 MHz and the

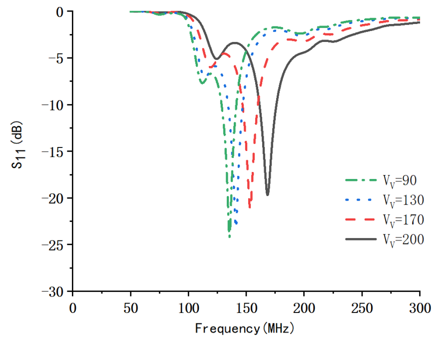

FIGURE 9. Simulated S_{11} with different values of v_V.

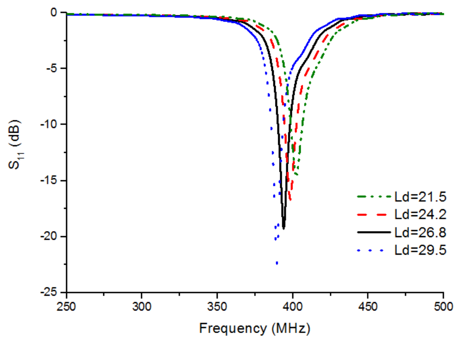

FIGURE 10. Simulated S_{11} with different values of L_d.

impedance bandwidth for VHF antenna is about 13 MHz. Simulation surface current distribution magnitude at the resonant frequencies of the UHF antennas is shown in Figure 8. It is obvious that the meander-line is mainly used to change the current path to achieve miniaturization. To investigate the effects of the VHF antenna length, the simulated S_{11} (dB) with different values of V_V is plotted in Figure 9. It shows that decreasing VHF antenna length causes the resonant frequency to shift upwards, and the impedance matching at lower frequencies becomes better. To investigate the effects of the last meander-line length, the simulated S_{11} as a function of L_d is shown in Figure 9. As the L_d increases, the resonant frequency tends to decrease and better impedance matching.

The radiation characteristics of the antenna are assessed considering the measured and simulated gain radiation patterns at the nominal operating frequency. The gain radiation patterns of the antenna with satellite structure are measured in far-field measurement systems. The gain radiation patterns of UHF/VHF antenna at 149 MHz and 398 MHz, illustrated in Figure 11. Even though the radiation patterns are distorted from an omnidirectional pattern at one or two angles, the omnidirectional features appears at most other frequencies. Due to the limited conditions in the anechoic chamber, only the UHF antenna was measured in the anechoic chamber. VHF antenna was measured outdoors. The measured gain is different from the simulated gain mainly influenced by the multipath effect.

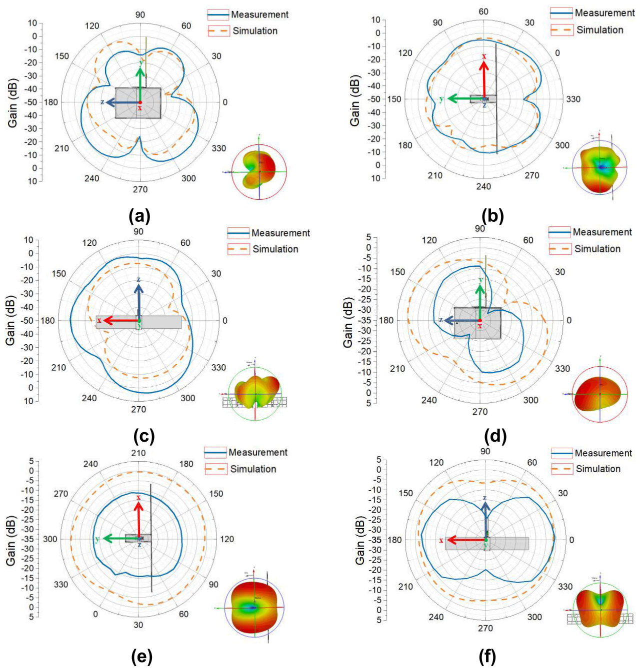

FIGURE 11. Simulated and measured radiation patterns (x-y, x-z and y-z planes) with satellite structure at 149 MHz and 398 MHz. (a) xoy plane of UHF (b) xoz plane of UHF (c) yoz plane of UHF (d) xoy plane of VHF (e) xoz plane of VHF (f) yoz plane of VHF.

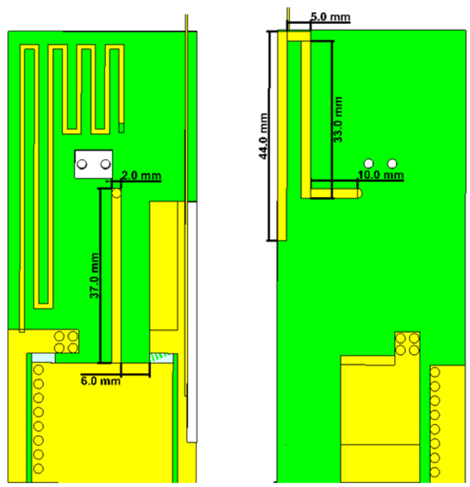

FIGURE 12. Decoupling structure.

IV. DECOUPLING STRUCTURE

Due to the close distance between the two monopole antennas, the coupling effect becomes very significant in UHF frequency band. In this part, a feasible decoupling structure is introduced and verified by simulation. A decoupling structure based on the antenna-ground branch decoupling principle is introduced. A new coupling path is introduced between the two antennas. In order to avoid VHF antenna contact decoupling structure, the decoupling structure is mostly placed on the back of the dielectric substrate, as shown in figure 12. By changing the length of the decoupling structure, a better isolation can be achieved at 398 MHz.

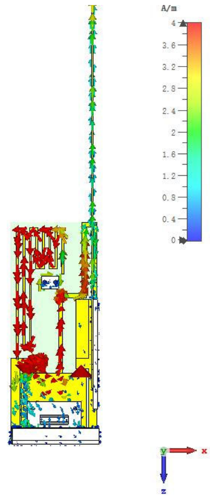

FIGURE 13. The current distribution of the antenna with decoupling structure at 398 MHz.

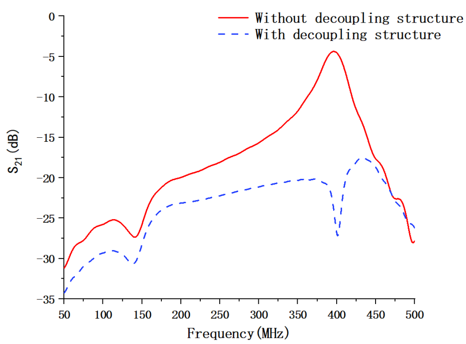

FIGURE 14. S_{21} curves with and without decoupling structure.

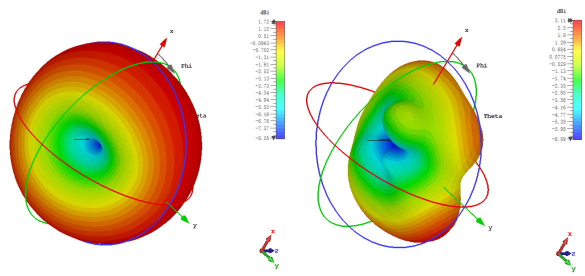

FIGURE 15. The direction diagram operating at 149 MHz and 398 MHz respectively.

After simulation verification, the S_{21} curve of proposed antenna is shown in Figure 14. The isolation degree of the two antennas decreased from −5 dB to −25 dB at 398 MHz.

Figure 13 shows the current distribution when the antenna works at 398 MHz after the decoupling structure is added. It can be seen from the figure that the coupling current in the VHF antenna decreases significantly. The coupling current generated by the decoupling structure on the VHF antenna is opposite to that generated by the UHF antenna on the VHF antenna. After optimization, the coupling current on the VHF antenna is effectively suppressed. Some

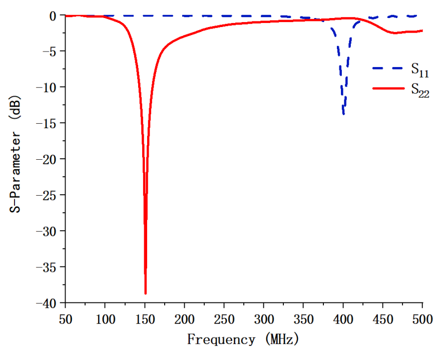

FIGURE 16. The S-parameter with decoupling structure.

TABLE 2. Comparison of characteristics of different VHF/UHF antenna.

Reference	Antenna type	Size	Operating frequency(MHz)	Antenna gain
[14]	Dual Band Printed Inverted F Antenna	304.8 mm × 22.86 mm × 6 mm	145 / 435	2.95 dBi at 145 MHz 5.06 dBi at 435 MHz
[15]	Deployable helix	500 mm	365	8 dB at 365 MHz
[16]	Dipole and Monopole Antennas	313.5 mm × 980 mm	144 / 435	2.02 dBi at 144 MHz 2.43 dBi at 435 MHz
[4]	Monopole	513.6 mm × 10 mm × 10 mm	146 / 438	2.06 dBi at 146 MHz 3.35 dBi at 438 MHz
[17]	Printed patch	320 mm × 80 mm × 3.17 mm	432	2.12 dB at 432 MHz
[18]	Modified PIFA	80 mm × 90 mm × 0.5 mm	450	0.6 dB at 450 MHz
Proposed antenna	Monopole	101 mm × 40 mm × 8.9 mm	149 / 398	1.72 dBi at 149 MHz 3.11 dBi at 398 MHz

performance of the proposed antenna changes as the introduction of decoupling structure. The antenna matching performance gets better as shown in figure 16. The gain of UHF antenna changed from 0.435 dBi to 3.11 dBi and the gain of VHF antenna changed from 1.58 dBi to 1.72 dBi as shown in figure 15. The size and performance of the proposed antenna was compared with existing VHF/UHF antennas, tabulated in Table 2. Considering the comparison criteria in the VHF/ UHF band, it can be seen that the proposed antenna was a potential candidate for the CubeSats communication system.

V. CONCLUSION

A new design of a compact integrated UHF/VHF antenna for CubeSats has been proposed in this paper. Compact size, low profile and geometric characteristics are realized in this design. The proposed antenna can work at UHF (398 MHz) and VHF (149 MHz) band. This design not only realizes the dual frequency work, but also allows the limitations of space for an antenna to be overcome. A decoupling structure is designed, and the antenna achieves better matching performance, lower coupling, and greater gain. So, the proposed antenna is a good approach for CubeSats.

REFERENCES

[1] H. Heidt, J. Puig-Suari, A. S. Moore, S. Nakasuka, and R. J. Twiggs, "CubeSat: A new generation of picosatellite for education and industry low-cost space experimentation," in *Proc. 14th Annu. Conf. Small Satell. (AIAA)*, Aug. 2001, pp. 1–19, Paper SSC00-V-5.
[2] Y. Rahmat-Samii, V. Manohar, and J. M. Kovitz, "For satellites, think small, dream big: A review of recent antenna developments for CubeSats," *IEEE Antennas Propag. Mag.*, vol. 59, no. 2, pp. 22–30, Apr. 2017.
[3] A. ALAmoudi and R. Langley, "Design of inverted F antenna for low earth orbit (LEO) satellite application," in *Proc. 3rd Eur. Conf. Antennas Propag.*, Berlin, Germany, Mar. 2009, pp. 1896–1899.
[4] T. F. C. Leao, V. Mooney-Chopin, C. W. Trueman, and S. Gleason, "Design and implementation of a diplexer and a dual-band VHF/UHF antenna for nanosatellites," *IEEE Antennas Wireless Propag. Lett.*, vol. 12, pp. 1098–1101, 2013.
[5] S. Gao, K. Clark, M. Unwin, J. Zackrisson, W. A. Shiroma, J. M. Akagi, K. Maynard, P. Garner, L. Boccia, G. Amendola, G. Massa, C. Underwood, M. Brenchley, M. Pointer, and M. N. Sweeting, "Antennas for modern small satellites," *IEEE Antennas Propag. Mag.*, vol. 51, no. 4, pp. 40–56, Aug. 2009.
[6] R. Wilke, M. Reiffenrath, K. Parow-Souchon, and D. Heberling, "S-band, UHF and VHF communication system for CubeSats including ground station software," in *Proc. 8th Pico-Nano-Satell. Workshop Technol. Small Satell. Res.*, 2015, pp. 1–21.
[7] M. T. Islam, S. C. P. Saisutjarit, S. Srikisuwan, D. Saenthawee, P. Akkaraekthalin, and S. Kuntanapreeda, "KNACKSAT-CubeSat project and the iniation of Thai aerospace industry," in *Proc. Thailand-Japan Microw. (TJMW)*, Bangkok, Thailand, 2016.
[8] A. Narbudowicz, S. Chalermwisutkul, P. J. Soh, M. F. Jamlos, and M. J. Ammann, "Compact UHF antenna utilizing CubeSat's characteristic modes," in *Proc. 13th Eur. Conf. Antennas Propag. (EuCAP)*, Krakow, Poland, Mar./Apr. 2019, pp. 1–3.
[9] M. J. Veljovic and A. K. Skrivervik, "Patch antenna system for CubeSats in L band," in *Proc. 13th Eur. Conf. Antennas Propag. (EuCAP)*, Krakow, Poland, Mar./Apr. 2019, pp. 1–5.
[10] M. Samsuzzaman, M. T. Islam, S. Kibria, and M. Cho, "BIRDS-1 CubeSat constellation using compact UHF patch antenna," *IEEE Access*, vol. 6, pp. 54282–54294, 2018.
[11] J. Buckley, D. Gaetano, L. Loizou, C. O'Mathuna, K. G. McCarthy, and B. O'Flynn, "Compact 433 MHz antenna for wireless smart system applications," *Electron. Lett.*, vol. 50, no. 8, pp. 572–574, Apr. 2014.
[12] A. Loutridis, M. J. Ammann, and M. John, "Folded meander line antenna for wireless M-bus in the VHF and UHF bands," *Electron. Lett.*, vol. 51, no. 15, pp. 1138–1140, Jul. 2015.
[13] J. Costantine, Y. Tawk, and C. G. Christodoulou, "Deployable antenna concepts for CubeSats," in *Proc. IEEE Int. Symp. Antennas Propag. (APSURSI)*, Fajardo, Puerto Rico, Jun. 2016, pp. 1541–2542.
[14] M. U. Khan, M. Maqsood, and A. I. Najam, "Dual band printed inverted f antenna (IFA) for low Earth orbit (LEO) small satellites," in *Proc. Int. Symp. Recent Adv. Electr. Eng. (RAEE)*, Islamabad, Pakistan, Oct. 2017, pp. 1–5.
[15] J. Costantine, Y. Tawk, I. Maqueda, M. Sakovsky, G. Olson, S. Pellegrino, and C. G. Christodoulou, "UHF deployable helical antennas for CubeSats," *IEEE Trans. Antennas Propag.*, vol. 64, no. 9, pp. 3752–3759, Sep. 2016.
[16] K. Schraml, A. Narbudowicz, S. Chalermwisutkul, D. Heberling, and M. J. Ammann, "Easy-to-deploy LC-loaded dipole and monopole antennas for CubeSat," in *Proc. 11th Eur. Conf. Antennas Propag. (EUCAP)*, Paris, France, Mar. 2017, pp. 2303–2306.

[17] X. Liu, D. R. Jackson, J. Chen, J. Liu, P. W. Fink, G. Y. Lin, and N. Neveu, ''Transparent and nontransparent microstrip antennas on a CubeSat: Novel low-profile antennas for CubeSats improve mission reliability,'' *IEEE Antennas Propag. Mag.*, vol. 59, no. 2, pp. 59–68, Apr. 2017.
[18] T. Alam, M. T. Islam, M. A. Ullah, and M. Cho, ''A solar panel-integrated modified planner inverted F antenna for low Earth orbit remote sensing nanosatellite communication system,'' *Sensors*, vol. 18, no. 8, p. 2480, Jul. 2018.

XIANG ZHANG received the Ph.D. degree in aeronautical and astronautical manufacturing from the Nanjing University of Aeronautics and Astronautics (NUAA), Nanjing, China, in 2006.

From 2007 to 2011, he was with the Mini-satellite Research Center, Nanjing University of Aeronautics and Astronautics, where he was the Associate Chief System Engineer of the TX-1 mini-satellite being in charge of the satellite system design, structural and thermal control design, and assembly and integration testing (AIT). Since January 2012, he has been with the Nanjing University of Science and Technology (NJUST), Nanjing, China, where he is currently an Associate Professor with the School of Mechanical Engineering and the Dean of the Mini/Micro Satellite Center, NJUST. He is the Project Manager of a number of satellite projects organized by European QB50 committee, or funded by Chinese General Armament Department, the Chinese Astronautical Institutes and NJUST. He has taken in charge of the design and manufacture of several CubeSats, including NJUST-1(one of the 50 CubeSats in QB50 project), NJUST-2 (collaborated with Shanghai Mini-Satellite Research Institute), and Bayi-1 (the first high-school education satellite of China). His research interests are microsatellite technology, including system and structural design, vision-based navigation, and satellite antenna design.

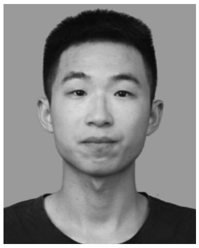

FU SUN received the B.Eng. degree from Binzhou University, Shandong, China, in 2019. He is currently pursuing the M.Eng. degree with the Nanjing University of Aeronautics and Astronautics, Nanjing, China. His current research interests include water antennas and slotted waveguide antenna.

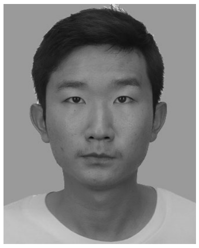

GUOXUAN ZHANG received the B.Eng. degree from the School of Civil Aviation University of China, Tianjin, China, in 2019. He is currently pursuing the M.Eng. degree with the Nanjing University of Aeronautics and Astronautics, Nanjing, China. His current research interests include water antennas and water filter.

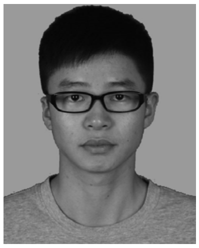

LIMING HOU received the B.E. degree from the Nanjing University of Science and Technology (NUST), Nanjing, China, in 2019, where he is currently pursuing the M.E. degree in space engineering. His current research interests include 3-D printed antennas and satellite networks.